


MIMO antenna for IOT devices with reconfigurable radiation pattern

Hyunwoong Shin  and Hyeongdong Kim
 Department of Electronics and Computer Engineering, Hanyang University, Seoul, Republic of Korea
 Email: hdkim@hanyang.ac.kr

Here, how to control isolation and correlation by adjusting the position of capacitors in a resonance structure in a MIMO ground radiation antenna is studied. The MIMO system consisting of two 7 mm × 7 mm printed ground radiation antennas operating at WLAN on a 40 mm × 40 mm ground plane was installed. If the positions of the capacitors of the two antennas are equally on the top of the ground plane, S_{12} is -5.2 dB and envelope correlation coefficient is 0.47. When the capacitors are orthogonal to each other, S_{12} is improved to -16.5 dB and envelope correlation coefficient is improved to 0.12. The orthogonality of the characteristic mode of the ground plane by the antennas is confirmed by the radiation patterns when the position of the capacitor is orthogonal.

Introduction: The MIMO antenna basically requires high isolation and low correlation performance. Physically, as the distance between the antennas increases, the isolation performance improves. However, for low correlation performance, it is necessary to adjust the radiation pattern [1–3]. A paper [4] that controls the radiation pattern of a ground radiation antenna is a good previous study for MIMO ground radiation antenna design. However, it analysed only a single antenna. The ground radiation antenna has a great advantage in implementing the MIMO antenna because it can change the characteristic mode of the ground plane by changing the position of the capacitor without changing the shape of the antenna. In this letter, we have studied the influence of the position of the capacitor in the resonance structure of the MIMO ground radiation antennas for high isolation and low correlation in the WLAN band.

Antenna design: Figure 1a shows a 7 mm × 7 mm ground radiation antenna located on the edge of a 40 mm × 40 mm ground plane on a 1-mm-thick flame retardant 4-type (FR-4) dielectric. The distance between the two antennas is 26 mm, which is approximately 0.21 λ at 2.45 GHz. The distance between the two antennas was set to 0.25 λ or less to observe the proposed antenna isolation change fairly. Each ground radiation antenna consists of a feed structure including capacitor C_F to control the input impedance and a resonance structure including capacitor C_R to control the resonance frequency [5–8]. There are three cases where the positions of C_R of antenna 1 and antenna 2 are different. In case 1, C_{R1} and C_{R2} are located on the top of the ground plane as shown in Figure 1b. In case 2, C_{R1} is located on the left side of the ground plane, and C_{R2} is located on the right side of the ground plane as shown in Figure 1c. In case 3, C_{R1} is located on the top of the ground plane, and C_{R2} is located on the right side of the ground plane as shown in Figure 1d.

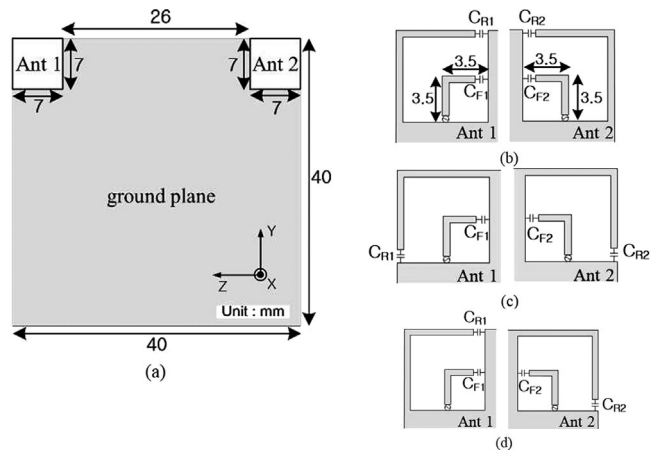


Fig. 1 Geometries of the proposed antennas

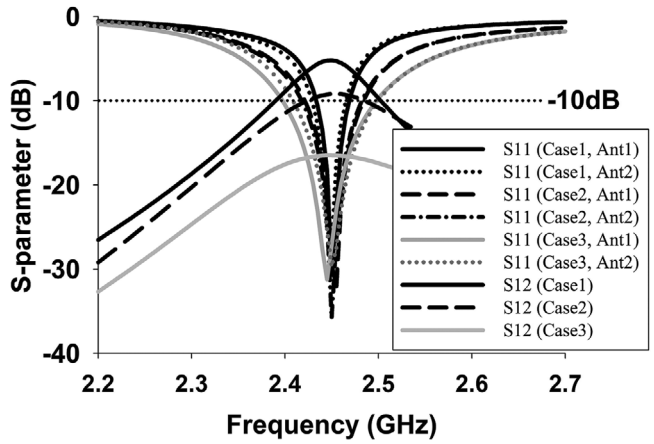


Fig. 2 Simulated S -parameters of the two antennas

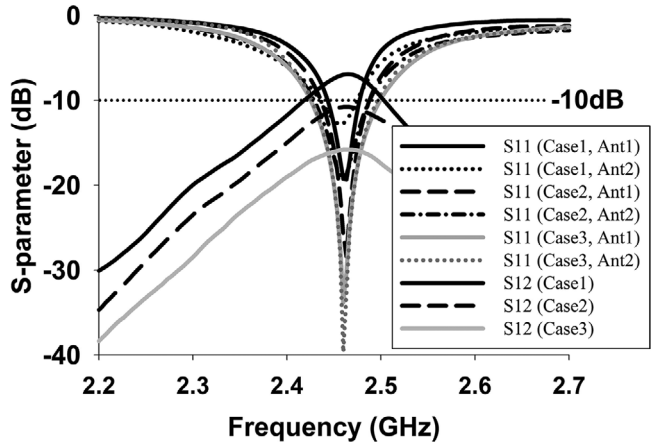


Fig. 3 Measured S -parameters of the two antennas

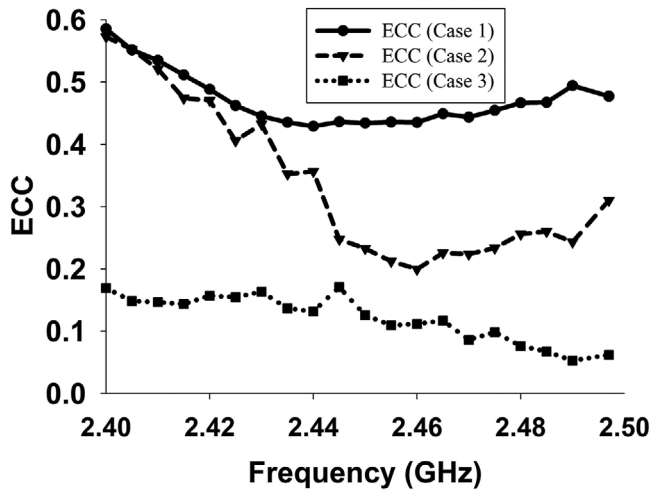


Fig. 4 Measured envelop correlation coefficient

case 3, C_{R1} is located on the top of the ground plane, and C_{R2} is located on the right side of the ground plane as shown in Figure 1d.

Simulation and measured results: Figure 2 shows simulated S -parameters of the two antennas in all three cases. All antennas are set to centre frequency of 2.45 GHz. The transmission coefficient (S_{12}) at 2.45 GHz in case 1 is -5.2 dB, in case 2 is -9.2 dB, and in case 3 is -16.5 dB. The -10 dB impedance bandwidth of both antennas is 40 MHz in case 1, 60 MHz in case 2, and 100 MHz in case 3. The impedance bandwidth for three cases are different because of the mutual coupling between the antennas. Figure 3 shows measured S -parameters, which are in good agreement with the simulation results. S_{12} of case 1 is -7 dB, S_{12} of case 2 is -10.8 dB, and case 3 is -15.8 dB.

Figure 4 shows the measured envelope correlation coefficient (ECC) values using the 3D cellular telecommunications industry association

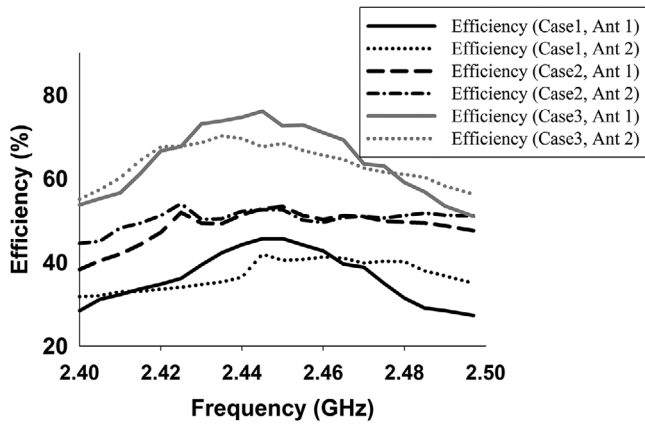


Fig. 5 Measured total efficiency

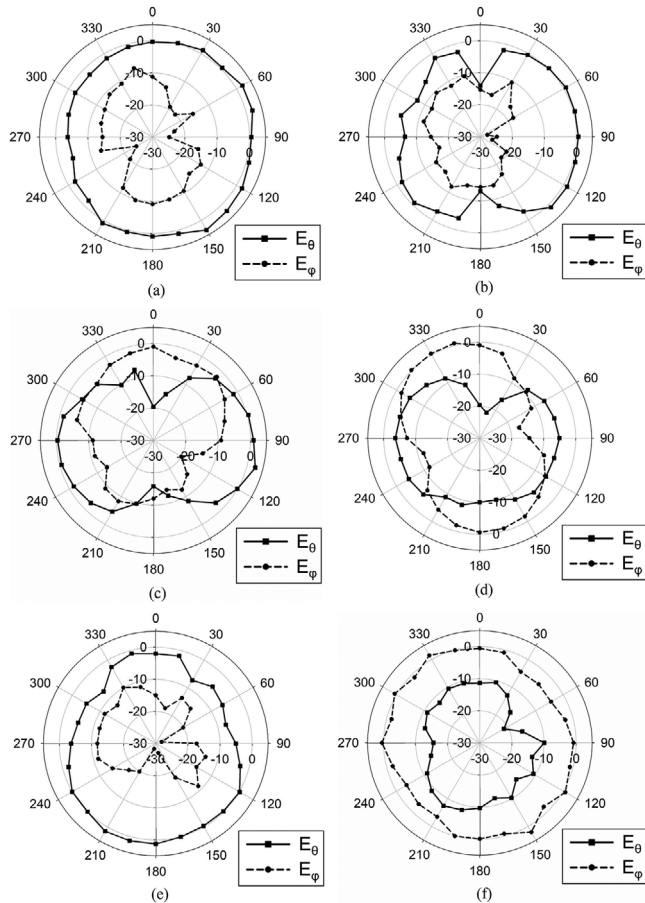


Fig. 6 Radiation patterns of antenna 1 and antenna 2 at 2.45 GHz

(CTIA) over-the-air (OTA) chamber. The average of ECC of case 1 is 0.47, of case 2 is 0.34, and of case 3 is 0.12. Case 3 has the lowest ECC values of less than 0.2 at all frequencies in the 2.4–2.5 GHz band and has the best MIMO performance. Figure 5 shows the measured total efficiencies of the MIMO antennas for each case. The antennas of case 1 have an average efficiency of 35% in the 2.4–2.5 GHz band. The antennas of case 2 have an average efficiency of 49% and case 3 have the average efficiency of 64%. The antennas of case 3 have the highest efficiency, and the antennas of case 1 have the lowest efficiency because of isolation loss.

Figure 6 shows the radiation patterns of case 3 where the positions of capacitor C_R of antenna 1 and antenna 2 are different at 2.45 GHz. Firstly, looking at the radiation patterns of antenna 1 where the capacitor is located on the top of the ground. In the XY -plane, the theta polarization of the electric field (E_θ) is omnidirectional and is stronger than the phi polarization of the electric field (E_ϕ) shown as Figure 6a. In the YZ -plane, the E_θ is about 15 dB stronger along the Y -axis direction than the Z -axis direction as shown in Figure 6b. In the XZ -plane, the E_θ is about 20 dB

stronger along the X -axis direction than the Z -axis direction as shown in Figure 6c. That is, antenna 1 of case 3 has the same radiation pattern as a Z -axis dipole-type antenna.

Secondly, we observed the radiation patterns of the antenna 2 in case 3 having capacitor C_R positioned on the right side of the ground plane. In the XY -plane, the E_ϕ is about 15 dB stronger along the X -axis direction than Y -axis direction as shown in Figure 6d. In the YZ -plane, the electric field is about 5 dB stronger along the Z -axis direction than the Y -axis direction as shown in Figure 6e. In the XZ -plane, the E_ϕ is the omnidirectional pattern as shown in Figure 6f. Therefore, antenna having capacitor C_R positioned on the side of ground plane has same radiation pattern as a Y -axis dipole-type antenna.

Conclusion: The ground radiation antenna changes the characteristic mode of the ground plane depending on the position of the capacitor in the resonance structure. In this letter, we studied the isolation and ECC of two ground radiation antennas depending on the position of the capacitor. When the capacitor is located on the top of the ground plane, the Z -axis dipole-type characteristic mode is mainly excited. When the capacitor is located on the side of the ground plane, the Y -axis dipole-type characteristic mode is mainly excited. Therefore, isolation and ECC performances are best when the capacitor is in the orthogonal position. All these results can be applied regardless of the size of the ground or the position of the antennas, and can be applied to applications in different frequency bands.

Acknowledgements: This work was supported by the National Research Foundation of Korea (NRF), grant funded by the Korean Government (MSIT) (No. 2019R1F1A1063993).

Conflict of interest: The authors have no potential conflict of interest pertaining to this submission to *Electronics letters*.

Data availability statement: Data openly available in a public repository that issues datasets with DOIs.

© 2022 The Authors. *Electronics Letters* published by John Wiley & Sons Ltd on behalf of The Institution of Engineering and Technology

This is an open access article under the terms of the Creative Commons Attribution-NonCommercial License, which permits use, distribution and reproduction in any medium, provided the original work is properly cited and is not used for commercial purposes.

Received: 6 December 2021 Accepted: 17 December 2021
doi: 10.1049/ell2.12423

References

- Li, H., Lau, B.K., Ying, Z., He, S.: Decoupling of multiple antennas in terminals with chassis excitation using polarization diversity, angle diversity and current control. *IEEE Trans. Antennas Propag.* **60**(12), 5947–5957 (2012)
- Zhang, S., Glazunov, A.A., Ying, Z., He, S.: Reduction of the envelope correlation coefficient with improved total efficiency for mobile LTE MIMO antenna arrays: mutual scattering mode. *IEEE Trans. Antennas Propag.* **61**(6), 3280–3291 (2013)
- Won, J., Jeon, S., Nam, S.: Identifying the appropriate position on the ground plane for MIMO antennas using characteristic mode analysis. *J. Electromag. Eng. Sci.* **16**(2), 119–125 (2016)
- Zhang, R., Liu, Y., Kim, H.: Effect of capacitor position on radiation patterns of ground radiation antenna. *Electron. Lett.* **51**(23), 1844–1846 (2015)
- Liu, Y., Lu, X., Jang, H., Choi, H., Jung, K., Kim, H.: Loop-type ground antenna using resonated loop feeding, intended for mobile devices. *Electron. Lett.* **47**(7), 426–427 (2011)
- Qu, L., Zhang, R., Shin, H., Kim, J., Kim, H.: Performance enhancement of ground radiation antenna for Z-wave applications using tunable metal loads. *Electron. Lett.* **52**(22), 1827–1828 (2016)
- Qu, L., Zhang, R., Shin, H., Kim, J., Kim, H.: Mode-controlled wideband slot-fed ground radiation antenna utilizing metal loads for mobile applications. *IEEE Trans. Antennas Propag.* **65**(2), 867–872 (2017)
- Zahid, Z., Kim, H.: Performance evaluation of loop-type ground radiation antenna based on its optimum impedance level. *Electron. Lett.* **53**(7), 446–448 (2017)